Semana Nacional de Engenharia Nuclear e da Energia e Ciências das Radiações - VII SENCIR
Belo Horizonte, 12 a 14 de novembro de 2024

Id.: EN-28

NEUTRONIC EVALUATION OF THE FUEL BURNUP DURING THE LIFETIME OF SEALER NUCLEAR REACTOR

Jefferson Q. C. Duarte, Thalles O. Campagnani, Cláubia Pereira, Clarysson A. M. Silva

Universidade Federal de Minas Gerais - UFMG, Av. Pres. Antônio Carlos, 6627, Escola de Engenharia, Bloco 4, DEN - Pampulha, Belo Horizonte - MG, Brasil. 31270-901
jefferson9@ufmg.br

Keywords: SEALER, Small Modular Reactor, Lead-coolant Reactor, Burnup, OpenMC

ABSTRACT

This paper presents a neutronic analysis of the SEALER (Swedish Advanced Lead Reactor), a fast Small Modular Reactor (SMR), comparing Uranium Dioxide (UO_2) and Uranium Mononitride (UN) fuels with equal enrichment under full-power conditions throughout the reactor's lifetime. A SEALER model was developed and validated against reference data. The evaluation of these fuels focuses on key parameters such as fuel burnup, the reactor's conversion ratio (CR), fuel isotopic composition, capture-to-fission ratio (α) and average number of neutrons produced per absorption (η) in significant nuclides, including $^{235}\mathrm{U}$ and $^{239}\mathrm{Pu}$. Simulation results reveal that UN fuel extends the reactor core's operational life and offers a slight advantage in neutron production from fissile nuclides. However, UO_2 achieves higher burnup, indicating more efficient energy extraction per ton of fuel. Additionally, UO_2 produces more plutonium per ton of uranium, aiding in the sustenance of the chain reaction and potentially reducing $^{235}\mathrm{U}$ consumption as burnup progresses. This is further supported by a greater value of α for $^{238}\mathrm{U}$ in UO_2 and higher CR values throughout the reactor's life. Thus, UN does not demonstrate a significant advantage when used with the same enrichment as UO_2. Consequently, UO_2 outperforms UN in the SEALER reactor configuration when UN is employed with its higher-density pellet and identical enrichment and geometry. All simulations were conducted using the OpenMC Monte Carlo code, with nuclear data libraries generated by NJOY21 at SEALER's operational temperatures. Matplotlib was utilized for data analysis and plotting relevant nuclide cross-sections at specific temperatures.

1. INTRODUCTION

The use of lead as a coolant in fast reactor systems offers notable safety advantages. Its boiling point of $2010\,\mathrm{K}$ is higher than that of sodium ($1156\,\mathrm{K}$) and lead-bismuth ($1943\,\mathrm{K}$), providing a greater safety margin in case of accidents and allowing operation at higher temperatures. Additionally, lead alloys do not react exothermically with water and air, as sodium does. Its high density-temperature gradient enables passive natural convection for residual heat removal, and its shielding properties against ionizing radiation help protect the vessel from significant neutron radiation damage [1]. Among the drawbacks, the most notable is the corrosion of structural materials. However, specific aluminum alloys have been researched for decades to address this issue, with promising results [2], [3].

SEALER (Swedish Advanced Lead-Cooled Reactor) is an $8\,\mathrm{MW_t}$ fast SMR that uses $19.75\,\%$ enriched uranium oxide fuel and lead as coolant. The reactor project aims to meet the demands for commercial power at remote regions such as the Arctic regions of Canada. Hence, it has been designed with a core life of 30 years assuming an availability of $90\,\%$ [4].

Such projects are particularly relevant in large countries like Brazil, which also require energy production in remote areas. *AMAZUL* acknowledges the potential benefits of SMRs, considering their

compact size and high power output [5]. Research on these types of reactors is important for Brazil to develop its own long-life reactor core, potentially using Accident Tolerant Fuels (ATF). These fuels, such as UN and U_3Si_2, have been tested experimentally and exhibit superior thermophysical properties compared to UO_2. In brief, they have higher density and thermal conductivity while maintaining a suitable melting temperature range [6]. Enhanced thermal conductivity improves fuel performance in extreme temperature conditions, potentially reinforcing the reactor's safety systems beyond current standards observed in conventional nuclear reactors. Therefore, the potential use of UN fuel in SEALER could further enhance the inherent safety of the reactor, offering improved resilience in high-temperature accident scenarios.
With this in mind, the present study evaluates the neutronic performance of UN fuel in SEALER, using equal enrichment, across the reactor's operational lifetime under full-power conditions. For comparison, the conventional UO_2 fuel is also simulated. OpenMC, a community-developed Monte Carlo neutron and photon transport code, was used to perform all simulations presented in this work [7].

2. METHODOLOGY

2.1. Model configuration

The *OpenMC* model, based on Wallenius, Qvist, Mickus, *et al.* [4] is presented in Fig. 1. Regarding material composition, the data are taken from reference [2], [4], [8]–[11]. The reactor core comprises 19 fuel assemblies, 12 control assemblies, 6 shutdown assemblies, 24 shield assemblies and 24 reflector assemblies. Fuel rod design includes an active fuel column, insulation pellets below and above the fuel column, an upper gas plenum, a lower shield, and end plugs at both extremities. Information about the fuels simulated and the fuel design parameters are given in Tab. 1. Average temperatures are set at 750 K for the fuel, 690 K for the fuel clad and 684 K for the coolant, in accordance with the reference. For the rest of the system, the average temperature is defined as 663 K, representing the minimum temperature of the system.

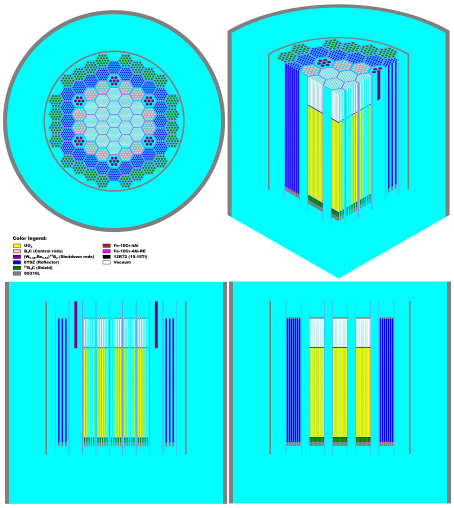

Figure 1. *OpenMC* model.

Item	Value
Power	8 MW_t
Enrichment	19.75%
UO_2 density (hot)	10.48 g/cm³
UO_2 composition (wt%)	$^{235}U_{17.4}$, $^{238}U_{70.72}$, $^{16}O_{11.84}$, $^{17}O_{0.004795}$, $^{18}O_{0.02672}$
UN density (hot)	13.74 g/cm³
UN composition (wt%)	$^{235}U_{18.65}$, $^{238}U_{75.78}$, $^{14}N_{5.5484}$, $^{15}N_{0.021833}$
Fuel assemblies	19
Fuel pins per assembly	91
Fuel pin pitch (hot)	16.37 mm
Fuel pellet diameter (hot)	13.40 mm
Fuel column height (hot)	1106 mm
Hex-can inner flat-to-flat	160 mm
Hex-can outer flat-to-flat	164 mm
Hex-can inner pitch	166 mm

Tab. 1. Fuel specification and design parameters.

2.2. Simulation settings

Different simulations were performed in *OpenMC 0.15.0*, the latest version available. paper. The control and shutdown rods are positioned aligned with the top of the fuel, representing the default position in the simulations. Steady-state simulations are configured for 400 cycles with 15000 particles per cycle, skipping 40 cycles. Burnup simulations are configured for 250 cycles with 10000 particles per cycle, considering 50 cycles skipped. These configurations were sufficient to maintain an error margin below 6% for all tallies computed.
Burnup calculations were divided into 730 steps of 15 days each, totaling 30 years of burnup. The *JEFF-3.1* and *ENDF\B-VIII.0* libraries were processed using NJOY21, via OpenMC's Python API, to generate microscopic cross sections at the desired operational temperatures. The *JEFF* library merely serves as a tool for model verification, as it was utilized in the reference work. Furthermore, the simplified chain CASL (fast spectrum) was chosen for describe the transmutation and decay channels, allowing depletion during the burnup [12]. It is important to note that there is no official chain file in OpenMC's repository specifically tailored for lead-cooled reactors. Therefore, a chain file designed for Sodium-cooled Fast Reactors (SFR), which applies capture branching ratios representative of an SFR spectrum to relevant isotopes, is utilized in this work. To solve the equation governing the transmutation of nuclides, *OpenMC* provides the use of various numerical methods, including CF4, which is based on a commutator-free Lie group integration method [13]. In this method, four transport solutions and five matrix exponentials are required per timestep. It has been chosen for its reliable performance compared to others high-order methods and its low error among explicit algorithms, hence converging well for larger time steps [14].

2.3. Phase 1 - Model validation

For model verification, the effective multiplication factor (k_{eff}), delayed neutron factor (β_{eff}) and shutdown margin (S_{dm}) are compared with the reference. These parameters were obtained considering an independent source located in the middle of the reactor. Performing k-eigenvalue calculation to obtain k_{eff} is pretty straightforward; however, two simulations are needed to get the mean value of β_{eff}. First, data from the first simulation is used to obtain k_{eff}. Second, another simulation is performed with only prompt neutrons. The equation to calculate the delayed neutron factor in pcm is then given by

$$\beta_{eff} = 1 - \frac{\text{Prompt Effective Multiplication Factor}}{\text{Effective Multiplication Factor}}. \tag{2.1}$$

The shutdown margin is evaluated by comparing the k_{eff} with all control and shutdown rods fully inserted to the k_{eff} with all rods fully withdrawn.

2.4. Phase 2 - Fuel burnup

According to Wallenius, Qvist, Mickus, *et al.* [4], SEALER's core was designed to operate for 30 years with a 90 % availability, equivalent to 9900 full power days. Consequently, burnup calculations were performed over this 30-year operational period to align with the project's original objectives. The following parameters are monitored at each time step of the fuel depletion:

- Effective neutron multiplication factor (k_{eff});
- Fission Reaction Rates (FRR) and Radiative Capture Reaction Rates (RCRR) in actinides;
- Fuel isotopic composition.

Fission products and actinides for each burnup step are displayed in Tab. 2. To avoid overloading the model with an excessive number of nuclides less relevant to the neutron balance, only the main fission products are tracked. Given that in fast reactors the likelihood of neutron capture by ^{239}Pu to form ^{240}Pu is lower than in thermal reactors, fewer higher actinides are produced. Therefore, the main actinides considered in the analysis are ^{235}U, ^{238}U, and ^{239}Pu.

Fission products	**Actinides**
^{81}Br, ^{78}Kr, ^{80}Kr, ^{82}Kr, ^{83}Kr, ^{84}Kr, ^{86}Kr, ^{89}Y, ^{90}Zr, ^{91}Zr, ^{92}Zr, ^{93}Zr, ^{94}Zr, ^{96}Zr, ^{95}Mo, ^{99}Tc, ^{101}Ru, ^{103}Ru, ^{103}Rh, ^{104}Pd, ^{105}Pd, ^{106}Pd, ^{108}Pd, ^{107}Ag, ^{109}Ag, ^{110}Cd, ^{111}Cd, ^{112}Cd, ^{113}Cd, ^{127}I, ^{129}I, ^{130}I, ^{128}Xe, ^{130}Xe, ^{131}Xe, ^{132}Xe, ^{134}Xe, ^{135}Xe, ^{136}Xe, ^{133}Cs, ^{134}Cs, ^{135}Cs, ^{136}Cs, ^{137}Cs, ^{141}Pr, ^{143}Nd, ^{145}Nd, ^{147}Nd, ^{148}Nd, ^{147}Pm, ^{148}Pm, ^{149}Pm, ^{147}Sm, ^{149}Sm, ^{150}Sm, ^{151}Sm, ^{152}Sm, ^{151}Eu, ^{152}Gd, ^{154}Gd, ^{155}Gd, ^{156}Gd, ^{157}Gd, ^{158}Gd, ^{160}Gd, ^{165}Ho	^{232}U, ^{233}U, ^{234}U, ^{235}U, ^{236}U, ^{237}U, ^{238}U, ^{235}Np, ^{236}Np, ^{237}Np, ^{238}Np, ^{239}Np, ^{236}Pu, ^{237}Pu, ^{238}Pu, ^{239}Pu, ^{240}Pu, ^{241}Pu, ^{242}Pu, ^{243}Pu, ^{244}Pu, ^{246}Pu, ^{241}Am, ^{242}Am, ^{243}Am, ^{244}Am, ^{241}Cm, ^{242}Cm, ^{243}Cm, ^{244}Cm, ^{245}Cm, ^{246}Cm

Table 2. Fission product and actinide content within each burnup step.

2.4.1. Capture-to-fission ratio (α)

OpenMC provides the FRR and RCRR for all nuclides, allowing us to calculate the Capture-to-fission ratio at each simulation step. It is defined as

$$\alpha_i = \frac{\sigma_{c,i}}{\sigma_{f,i}} = \frac{\phi\, n_i\, \sigma_{c,i}}{\phi\, n_i\, \sigma_{f,i}} = \frac{RCRR_i}{FRR_i}. \tag{2.2}$$

Here, ϕ represents the average flux in fuel cells and n_i the nuclide density, while $\sigma_{c,i}$ and $\sigma_{f,i}$ denote the capture and fission microscopic cross sections for each nuclide i, respectively. In *OpenMC*, this is accomplished directly by acquiring the FRR and RCRR for each nuclide i.

2.4.2. Conversion ratio (CR)

CR is the conversion process of fertile nuclides into fissile nuclides. In a fast reactor, where the average energy of neutrons is high, it can potentially maintain a CR higher than unity. In this situation, CR is called breeding ratio (BR). It is defined as the ratio of fissile material produced (FP) to the fissile ratio material destroyed (FD). For calculate CR in *OpenMC*, the equation is given by

$$CR = \frac{FP}{FD} = \frac{C_{fertile}}{(C_{fissile} + F_{fissile})}, \tag{2.3}$$

where $C_{fertile}$ represents the RCRR in fertile nuclides, $C_{fissile}$ RCRR in fissile nuclides and $F_{fissile}$ the FRR in fissile nuclides. As mentioned previously, the production of other fertile nuclides such as ^{240}Pu is very low, and for this reason, only ^{238}U is considered among fertile nuclides. Similarly, for fissile nuclides, only ^{235}U and ^{239}Pu are taken into account.

2.4.3. Average neutrons produced per absorption (η)

η_i is defined as the average neutrons produced per absorption in each nuclide i. The η equation for the main actinides is defined as

$$\eta_i = \frac{\nu_i}{(1+\alpha_i)}, \tag{2.4}$$

where ν_i represents the average neutrons produced per fission of nuclide i, and α_i is the capture-to-fission ratio in each nuclide i. This equation provides a measure of the neutron economy for each actinide by accounting for both neutron production and neutron losses through capture. A higher η indicates a better neutron economy. More neutrons are produced per absorption, and these neutrons can potentially refuel the reactor by fissioning fissile nuclides and being captured by fertile nuclides.

2.4.4. Fuel isotopic composition

The changes in the fuel isotopic composition are determined by the mass variation of each nuclide i between the beginning-of-cycle (BOC) and end-of-cycle (EOC) is given by

$$M_i = M_{i,EOC} - M_{i,BOC}. \tag{2.5}$$

3. RESULTS

3.1. Phase 1 - Model validation

The *OpenMC* model is verified from data present in Tab. 3, which compares the effective multiplication factor (k_{eff}), delayed neutron factor (β_{eff}) and shut-down margin (S_{dm}) with those reported in the reference work, where UO_2 fuel is used.

Item	k_{eff}	β_{eff} (pcm)	S_{dm} (pcm)
Reference (Serpent version 1.18)	1.04712	752	-3000
OpenMC model	1.04816 ± 0.00031	723 ± 37	-3009 ± 31

Table 3. Comparison of neutronic parameters with the reference [4].

The difference in k_{eff} is observed approximately at the fourth decimal place ($\Delta k_{eff} = 104$ pcm), while β_{eff} and S_{dm} difference remain within their own statistical margins ($\Delta\beta_{eff} = 29$ pcm and $\Delta S_{dm} = 9$ pcm, respectively). Hence, there is no significant difference, indicating that the model was well-defined.

3.2. Phase 2 - Fuel burnup

At this stage of the study, the neutronic behavior of UN and UO_2 fuels is examined without any modifications to the geometry or initial enrichment. This includes direct and indirect investigations of reactivity, cross sections, reaction rates, and fuel composition.

3.2.1. Reactivity evaluation

As showed in Fig. 2, in the initial state, there is a k_{eff} difference of 6940 pcm between UN and UO_2. At this specific case, this discrepancy is expected given that UN is a high-density fuel, which means more fissile material available. The reactivity loss over 30 years of burnup under full power

conditions is 2992 pcm and 4321 pcm, for UN and UO_2 respectively. Therefore, UN fuel extends the life of the reactor core. At the end of the reactor's life, UN achieves a maximum burnup of 25 GWd/tU, compared to 35 GWd/tU for UO_2, indicating that UO_2 is more efficient in extracting energy per ton of fuel. To achieve the same burnup with UN fuel, an increase in operation time is necessary. This results in the fuel being irradiated for a longer period, leading to greater physical damage to the material's structure and higher overall radioactivity.

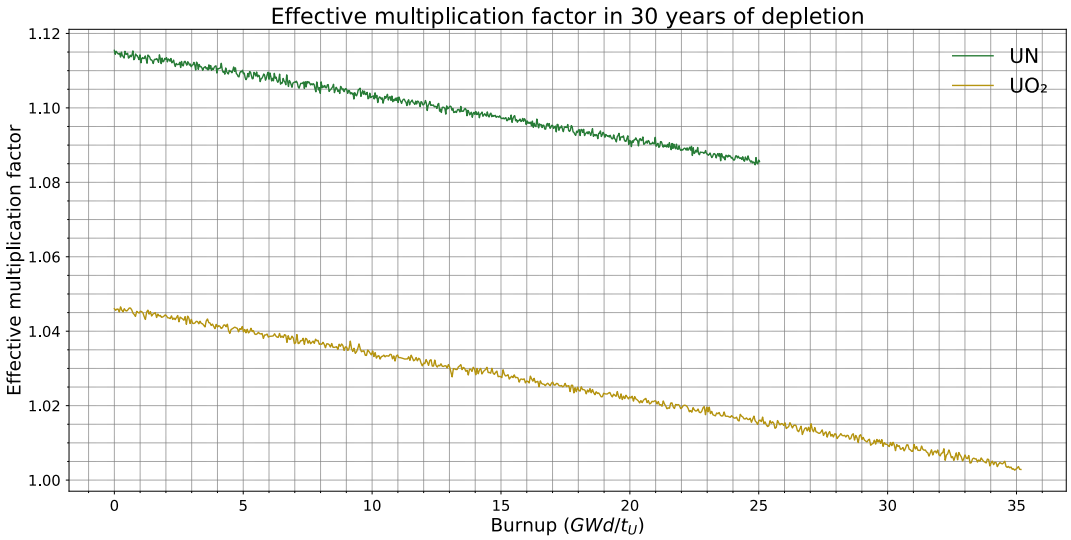

Figure 2. Effective multiplication factor during fuel burnup in SEALER.

Before delving deeper into other simulation results, it is important to emphasize how significant this reactivity difference is in SEALER's configuration. For the UN, k_{eff} with all control and shutdown rods inserted is 1.05110 ± 0.00031. So, using UN fuel with equal enrichment makes it impossible to shut down the system without developing new absorber rods or making modifications to certain assembly designs. As a burnup study, this does not impact the current work, but future research may consider adjustments to address this issue.

3.2.2. Cross sections and reaction rates

The evaluation of cross sections and reaction rates is essential for understanding the isotopic evolution of fuels according to reactor physics. Taking this into account, Fig. 3 presents the total scattering and absorption cross sections for both nitrogen and oxygen, and as seen the scattering cross section is more predominant in ^{16}O than in ^{14}N around 0.1 to 1 MeV, where most fissions occurs. However, in the case of the absorption cross section, the situation reverses, showing a much higher relevance in ^{14}N.

Given Fig. 4, a lower number of scattering reactions in ^{14}N indicates a harder flux spectrum. The radiative capture reaction rates (RCRR) depends on several factors, such as which nuclide it interacts with, neutron energy, the total mass of the nuclides, and the average neutron flux in the studied region. With that in mind, a lower average flux in UN fuel can be sufficient to result in a lower radiative capture rate, even considering its higher mass of ^{238}U. As can be seen in Tab. 4 and Tab. 5,

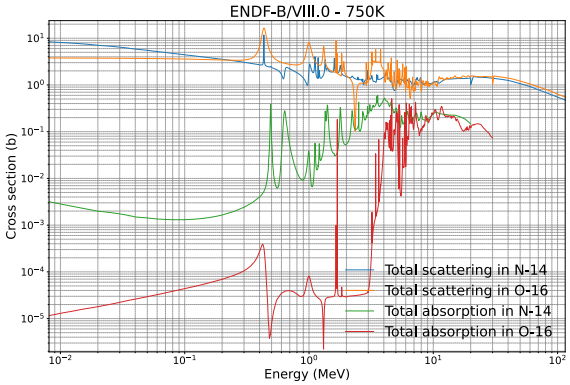

Figure 3. Scattering and absorption cross sections in ^{16}O and ^{14}N at 750K.

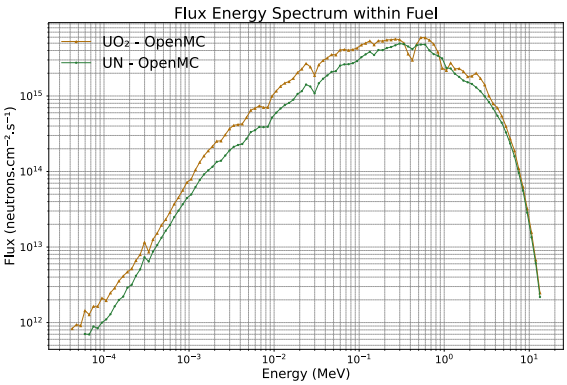

Figure 4. Flux energy spectrum of both fuels at BOC within a 6% margin of error.

the average capture-to-fission ratio (α) for the ^{235}U and ^{239}Pu is higher in UO_2, while the average neutrons produced per absorption (η) is lower.

Nuclides	**UO_2**		**UN**	
	BOC	**EOC**	**BOC**	**EOC**
^{235}U	0.2518	0.2561	0.2321	0.2352
^{239}Pu	-	0.2073	-	0.1722
^{238}U	4.2612	4.5056	3.6126	3.7566

Table 4. Average α_i of ^{235}U, ^{238}U and ^{239}Pu in both fuels.

Nuclides	**UO_2**		**UN**	
	BOC	**EOC**	**BOC**	**EOC**
^{235}U	1.9720	1.9638	2.0103	2.0041
^{239}Pu	-	2.4466	-	2.5255
^{238}U	0.5186	0.4957	0.5931	0.5750

Table 5. Average η_i of ^{235}U, ^{238}U and ^{239}Pu in both fuels.

This indicates that UO_2 has a poorer neutron economy, a term that represents the analysis of fissile material efficiency during the chain reaction. A higher α for ^{235}U and ^{239}Pu means that more neutrons are lost by RCRR in the fissile nuclides, and a lower η signifies fewer neutrons are available per absorption for sustaining the chain reaction. Regarding the fertile nuclide, ^{238}U, both tables previously mentioned indicate a better production of ^{239}Pu in UO_2 due to a higher RCRR. This is further confirmed in Fig. 5, where the conversion ratio (CR) remains higher in UO_2 throughout the reactor's lifetime.
It is also worth noting that the CR in both cases is less than 1, implying by definition that the SEALER was not designed to function as a breeder reactor.

3.2.3. Isotopic fuel evolution

The concentration of fission products, concerning absorbers, is nearly identical, as illustrated in Fig. 6. It is pertinent to note that the most significant fission product absorbers present in Fig. 6 are arranged in descending order from left to right. Additionally, other relevant fission products, such as ^{137}Cs, are not depicted here. The final inventory after 30 years of depletion is presented in Tab. 7.
Regarding the UO_2 fuel, since ^{239}Pu production predominates over other plutonium isotopes and the CR remained higher throughout the reactor's entire lifespan, we can conclude that this fuel generated more plutonium per ton of uranium mass. As ^{239}Pu increases more significantly in UO_2,

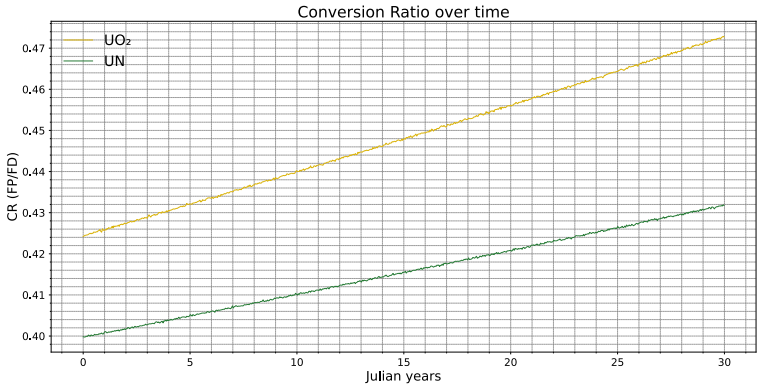

*A Julian year is a unit of time representing the duration of a year in the Julian calendar, equivalent to 365.25 days.

Figure 5. Conversion ratio over 30 years of burnup.

the fission rate of ^{235}U decreases, which may initially appear advantageous due to the preservation of this isotope. However, Tab. 6 shows that ^{235}U depletes at a higher rate when UO_2 is used as fuel, with a difference of 0.6%. The explanation for this lies in the RCRR of ^{235}U in UO_2, mentioned in the previous subsection. Despite this, the difference in ^{235}U loss is very small and does not provide a significant advantage in favor of using UN.

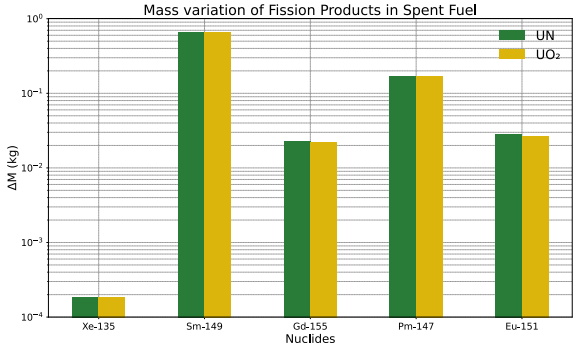

Figure 6. Concentration of the main fission products in spent fuel.

Item	U-235	U-238
UN		
Initial mass (kg)	6.91×10^2	2.81×10^3
Final mass (kg)	5.92×10^2	2.75×10^3
Mass lost (kg)	9.94×10^1	5.53×10^1
UO_2		
Initial mass (kg)	4.92×10^2	2.00×10^3
Final mass (kg)	3.92×10^2	1.94×10^3
Mass lost (kg)	1.00×10^2	5.90×10^1

Table 6. Mass inventory of ^{235}U and ^{238}U.

4. CONCLUSION

A neutronic analysis of fuel burnup in UO_2 and UN was conducted under full power conditions throughout the lifetime of SEALER. The simulation configurations are constrained by computational cost, which manifests in considerable stochastic fluctuations during burnup steps. Nevertheless, the geometry and material definitions are precise, and the overall behavior of the depletion curve remains unaffected. Consequently, the steady-state results align closely with reference data, and the precision of the depletion results is sufficient for making this comparison.
Simulation results of SEALER indicate that UN presents a high excess reactivity, making it impossible to have a shut-down margin and necessitating changes to the geometry or materials to operate

Nuclide	**UO_2 Fraction (wt%)**	**UN Fraction (wt%)**
^{235}U	16.3437	17.3798
^{238}U	80.9671	80.8631
^{237}Np	0.0285	0.0201
^{238}Pu	0.0015	0.0011
^{239}Pu	1.7919	1.2609
^{240}Pu	0.0345	0.0242
^{241}Pu	0.0004	0.0002
^{242}Pu	0.0000	0.0000
Total TRU fraction	1.8568	1.3065
Total actinide mass (ton)	2.4	3.4

Table 7. Actinide inventory in spent fuels, relative to total actinide content.

the reactor. The study also shows that the rate of reactivity loss as a function of burnup is lower, which extends the reactor core's operational life. These factors open the possibility for reducing enrichment of UN.

In UN, there is a slight advantage in neutron economy due to the lower radiative capture rate of ^{235}U; however, this is insufficient to preserve a significant quantity of ^{235}U in the fuel. On the other hand, UO_2 achieves higher burnup, demonstrating its superior capacity for energy extraction from fuel per ton. Additionally, it generates more plutonium per unit mass, which helps sustain the chain reaction, reducing ^{235}U comsumption as burnup increases.

From a neutronic perspective, UO_2 performs better in the SEALER reactor configuration when compared to a higher-density UN pellet with the same enrichment and geometry, due to its considerably higher burnup in relation to the initial uranium mass. Future work aims to study the neutronic viability of using UN with reduced ^{235}U enrichment by assessing the increase in ^{239}Pu generation and the reduction in ^{235}U consumption. This will allow adjust a adequate shutdown margin without the need for developing new absorber rods or make changes to the system's geometry.

ACKNOWLEDGEMENTS

The authors are grateful to the Brazilian research funding agencies: *Coordenação de Aperfeiçoamento de Pessoal de Nível Superior* (CAPES), *Fundação de Amparo à Pesquisa do Estado de Minas Gerais* (FAPEMIG) and *Conselho Nacional de Desenvolvimento Científico e Tecnológico* (CNPq) for the support. We would like to extend our gratitude to Prof. Dr. Carlos Velasquez for their support throughout this research endeavor.

References

[1] G. Sanchis Ramírez, "Safety-informed design of lead-cooled reactors on mobile platforms", M.S. thesis, Universitat Politècnica de Catalunya, 2022.

[2] J. Ejenstam, M. Halvarsson, J. Weidow, B. Jönsson, and P. Szakalos, "Oxidation studies of fe10cral–re alloys exposed to pb at 550 c for 10,000 h", *Journal of Nuclear Materials*, vol. 443, no. 1-3, pp. 161–170, 2013.

[3] J. Ejenstam and P. Szakálos, "Long term corrosion resistance of alumina forming austenitic stainless steels in liquid lead", *Journal of Nuclear Materials*, vol. 461, pp. 164–170, 2015.

[4] J. Wallenius, S. Qvist, I. Mickus, S. Bortot, P. Szakalos, and J. Ejenstam, "Design of sealer, a very small lead-cooled reactor for commercial power production in off-grid applications", *Nuclear Engineering and Design*, vol. 338, pp. 23–33, 2018.

[5] Amazônia Azul Tecnologias de Defesa S.A., *Plano de negócios 2024*, Tecnologia Nacional em Benefício da Sociedade, Acesso em: 30 de maio de 2024, 2024.

[6] J. K. Watkins, A. Gonzales, A. R. Wagner, E. S. Sooby, and B. J. Jaques, "Challenges and opportunities to alloyed and composite fuel architectures to mitigate high uranium density fuel oxidation: Uranium mononitride", *Journal of Nuclear Materials*, vol. 553, p. 153 048, 2021.

[7] P. K. Romano, N. E. Horelik, B. R. Herman, A. G. Nelson, B. Forget, and K. Smith, "Openmc: A state-of-the-art monte carlo code for research and development", *Annals of Nuclear Energy*, vol. 82, pp. 90–97, 2015.

[8] S. L. Hayes, "Material property correlations for uranium mononitride", Ph.D. dissertation, Texas A&M University, 1989.

[9] J. Wallenius, "Shutdown rod for lead-cooled reactors", *World Intellectual Property Organization (WIPO)*, 2017.

[10] W. K. Yoshito, V. Ussui, D. R. R. Lazar, and J. O. A. Pascoal, "Synthesis and characterization of nio-8ysz powders by coprecipitation route", in *Materials science forum*, Trans Tech Publ, vol. 498, 2005, pp. 612–617.

[11] S. S. Company, *316/316l/317l specification sheet*, Accessed: 2024-05-30, 2023. [Online]. Available: `https://www.sandmeyersteel.com/images/316316l/316-316l-317l-spec-sheet.pdf`.

[12] K. S. Kim, "Specification for the vera depletion benchmark suite", Dec. 2015. doi: `10.2172/1256820`. [Online]. Available: `https://www.osti.gov/biblio/1256820`.

[13] E. Celledoni, A. Marthinsen, and B. Owren, "Commutator-free lie group methods", *Future Generation Computer Systems*, vol. 19, no. 3, pp. 341–352, 2003.

[14] C. Josey, "Development and analysis of high order neutron transport-depletion coupling algorithms", Ph.D. dissertation, Massachusetts Institute of Technology, 2017.